ANNALS OF THE CHRYSENE FORMALISM
RESEARCH ARTICLE | AI-AUGMENTED PEER-REVIEWED | VOL. 1, NO. 5 | NOVEMBER 2026

Arithmetic Geometry, Spectral Zeta Theory, and Non-Commutative Geometry of the Chrysene Formalism

The (9, 8) Hermitian Curve over GF(4), Genus-1 Goppa Codes, the Ihara–Bass Zeta Function, and Connes' Spectral Triple

Charles D. Schaper, Ph.D.
Chief Editor, Annals of the Chrysene Formalism
San Francisco, California, USA
editor@chrysene.com

Abstract

Beyond its role in biogenesis and molecular quantum transport, the Chrysene Formalism defines an autonomous system of pure mathematics whose axioms are abstracted from the 18-vertex staggered C_{2h} graph G_{chr} (Article 40), the quaternary Galois field $\text{GF}(4) = \mathbb{F}_2[\omega]/(\omega^2 + \omega + 1)$ (Article 4, Theorem 9; Article 98), and the 3D cellular complex $B(n_x, n_y, n_z)$ (Article 80). This paper develops four theorems in arithmetic geometry, algebraic-geometry coding theory, spectral graph zeta theory, and Connes' non-commutative geometry that extend the coding constructions of Article 98 and develop mathematical counterparts to the programs in Article 4 and the conditional distance discussion of Article 90.

First, passing from the genus-0 projective line $\mathbb{P}^1(\text{GF}(4))$ (5 rational points) of Article 98 to the smooth projective genus-1 Hermitian curve $\mathcal{E}_H : Y^2Z + YZ^2 = X^3$ over GF(4) (with affine equation $y^2 + y = x^3$, i.e., $\text{Tr}_{\text{GF}(4)/\mathbb{F}_2}(y) = \text{N}_{\text{GF}(4)/\mathbb{F}_2}(x)$), we prove that $\mathcal{E}_H(\text{GF}(4))$ saturates the Hasse–Weil bound with equality: $|\mathcal{E}_H(\text{GF}(4))| = 4 + 1 + 2(1)\sqrt{4} = 9$ rational points (8 affine points plus $P_\infty = [0 : 1 : 0]$), forming the elementary abelian 3-torsion group $\mathbb{Z}_3 \times \mathbb{Z}_3$. The 9 rational points can, after a choice of bijections, index the 9 starred vertices V_A (and 9 unstarred vertices V_B) of $G_{\text{chr}} = (V_A \sqcup V_B, E)$, while the 8 non-trivial affine 3-torsion points have the same cardinality as the $K(G_{\text{chr}}) = 8$ Kekulé perfect matchings.

Second, evaluating the Riemann–Roch spaces $\mathcal{L}(mP_\infty)$ across the divisor $D = P_1 + \cdots + P_8$ of the 8 affine points of $\mathcal{E}_H(\text{GF}(4))$, we prove that $\mathcal{L}(4P_\infty) = \text{span}_{\text{GF}(4)}\{1, x, y, x^2\}$ defines a strictly Euclidean self-dual genus-1 Geometric Goppa code $C_{\text{Herm},4} = [8, 4, 4]_4$ (256 codewords, weight enumerator $1 + 18z^4 + 96z^5 + 24z^6 + 96z^7 + 21z^8$), while $\mathcal{L}(3P_\infty) = \text{span}_{\text{GF}(4)}\{1, x, y\}$ defines a double-error-correcting $[8, 3, 5]_4$ Goppa code (64 codewords, $d_{\min} = 5$), extending the genus-0 constructions associated with Article 98. Third, exact Laplacian cofactor calculations show that C_{2h} chrysene and D_{2h} tetracene to share the exact spanning-tree complexity $\kappa(G_{\text{chr}}) = \kappa(G_{\text{tet}}) = 1,189$ and Ihara–Bass derivative $P'_G(1) = 7,134$, whereas the bay-region step-defect raises the degree-shift Zagreb invariant from $\mathcal{I}_Q(\text{tet}) = 42$ to $\mathcal{I}_Q(\text{chr}) = 44$, splitting their 3-matching counts (816 vs. 814) and degree-6 Sachs zeta coefficients (−824 vs. −822). Fourth, we axiomatize the finite even spectral data with an antiunitary symmetry $(\mathcal{A}_C, \mathcal{H}_C, D_C, \gamma_C, J_C)$ and prove the Connes spectral distance bounds $d_{D_6} \geq 2.50$ and $d_{D_{54}} \geq 26.50$ in the explicit unit-hopping path model motivated by Article 90.

Keywords: Chrysene Formalism; pure mathematics; Hermitian curve over GF(4); Hasse–Weil bound; genus-1 Geometric Goppa codes; Ihara–Bass zeta function; spanning-tree complexity; Connes' spectral triple.

1 Introduction

1.1 The Chrysene Formalism as an axiomatic branch of pure mathematics

Across the foundational and synthesis articles of this series, the molecular structure of 3,6,9,12-tetrasubstituted chrysene and its 3D cellular assemblies has served two parallel objectives: proposing models of biogenesis and molecular quantum transport [Sch26a, Sch26e, Sch26j, Sch26c, Sch26g], and instantiating a self-contained system of pure mathematics [Sch26b, Sch26i, Sch26d, Sch26f, Sch26h]. Specifically:

(i) *Bipartite graph invariants (Article 40 [Sch26b]; Article 97 [Sch26f]):* The 18-vertex, 21-edge staggered C_{2h} graph $G_{\text{chr}} = (V_A \sqcup V_B, E)$ splits into two 9-vertex bipartite halves $|V_A| = |V_B| = 9$ and admits $K(G_{\text{chr}}) = 8$ Kekulé

Citation: Schaper, C. D. (2026). Arithmetic Geometry, Spectral Zeta Theory, and Non-Commutative Geometry of the Chrysene Formalism: The (9, 8) Hermitian Curve over GF(4), Genus-1 Goppa Codes, the Ihara–Bass Zeta Function, and Connes' Spectral Triple. *Annals of the Chrysene Formalism*, 1(5):1966–1974.
https://chrysene.com/index.php/acf/article/view/102
© 2026 Charles D. Schaper. Distributed under the Creative Commons Attribution-NonCommercial-NoDerivatives 4.0 International License. First published by Schaper Systems Press in the Annals of the Chrysene Formalism, Vol. 1, No. 5 (2026).

matchings ($\det A_{\text{chr}} = -64$), compared to $K(G_{\text{tet}}) = 5$ ($\det A_{\text{tet}} = -25$) for linear D_{2h} tetracene;

(ii) *Algebraic-geometry Goppa codes over* GF(4) *(Article 4, Theorem 9 & Appendix A.3 [Sch26a]; Article 98 [Sch26h]):* Article 98 constructed the genus-0 evaluation codes $[4, 2, 3]_4$ and $[5, 3, 3]_4$ on $\mathbb{P}^1(\text{GF}(4))$ and motivates extension to higher-genus Hermitian curves; and

(iii) *Non-commutative geometry and spectral triples (Article 4, Appendix A.1 [Sch26a]; Article 90, conditional distance discussion [Sch26i]):* Article 90 introduced the stacked quotient algebras $\mathcal{Q}_1$ (dim = 4) and $\mathcal{Q}_6$ (dim = 4,096) together with the Connes spectral distance lower bounds 2.50 ($l = 6$) and 26.50 ($N = 54$ in the path reduction of $B(3, 3, 6)$).

In this paper we abstract these structures into pure mathematics, proving four theorems that connect the Chrysene Formalism to arithmetic geometry over finite fields, Riemann–Roch Goppa coding theory, Ihara–Bass graph zeta theory, and Connes' non-commutative spectral geometry.

1.2 What is established here, by kind

Recovered. Article 4's Appendices A.1 and A.3 [Sch26a]; Article 40's 18-vertex bipartite graph G_{chr} [Sch26b]; Article 90's quotient algebra dimensions $(4, 4,096)$ and Connes distance bounds $(2.50, 26.50)$ [Sch26i]; Article 98's coding program [Sch26h].

Proved here. The $(9, 8)$ Hasse–Weil Saturation and Bipartite/Kekulé Correspondence Theorem on the genus-1 Hermitian curve $\mathcal{E}_H : Y^2Z + YZ^2 = X^3$ over GF(4), proving $|\mathcal{E}_H(\text{GF}(4))| = 9 = |V_A| = |V_B|$, $|\mathcal{E}_H^{\text{aff}}(\text{GF}(4))| = 8 = K(G_{\text{chr}})$, and $\mathcal{E}_H(\text{GF}(4)) \cong \mathbb{Z}_3 \times \mathbb{Z}_3$ (Theorem 3.2); construction of the genus-1 Hermitian Goppa codes $C_{\text{Herm},4} = [8, 4, 4]_4$ (strictly Euclidean self-dual, $C_{\text{Herm},4} = C_{\text{Herm},4}^{\perp}$, with weight enumerator $1 + 18z^4 + 96z^5 + 24z^6 + 96z^7 + 21z^8$) and $C_{\text{Herm},3} = [8, 3, 5]_4$ ($d_{\min} = 5$), extending the genus-0 constructions associated with Article 98 (Theorem 4.2); the graph-specific spanning-tree equality $\kappa(G_{\text{chr}}) = \kappa(G_{\text{tet}}) = 1,189$ ($P'_G(1) = 7,134$) and the degree-shift Zagreb splitting $\mathcal{I}_Q(\text{chr}) = 44 > \mathcal{I}_Q(\text{tet}) = 42$ separating the 3-matching counts (816 vs. 814) and Sachs zeta coefficients (−824 vs. −822; Theorem 5.1); axiomatic verification of the finite even spectral data with an antiunitary symmetry $(\mathcal{A}_C, \mathcal{H}_C, D_C, \gamma_C, J_C)$ and analytical proof of the Connes distance bounds 2.50 and 26.50 (Theorem 6.1).

2 Conventions, nomenclature, and non-implications

Convention 2.1 (Status labels)**.** Every numbered statement carries one of four labels: **[A]** finite or algebraic within the stated mathematical model; **[D]** derived under hypotheses named and registered in Appendix A; **[C]** imported from a cited source; **[E]** a physical or chemical reading, entering no proof. Reported finite invariants are checked by `verify_a102.py` (blocks Z1–Z6, Appendix B).

The labels classify mathematical rather than empirical claims. They do not mean that every theorem is formalized in Lean. Classical smooth-cubic genus, Riemann–Roch, Hasse–Weil, and Bass results are used in their standard forms; the companion dossiers state which finite consequences were executed and formally checked.

Notation 2.2 (Arithmetic-geometric, zeta, and spectral objects)**.** $\text{GF}(4) = \{0, 1, \omega, \omega^2\}$ with Frobenius involution $\bar{z} = z^2$, absolute trace $\text{Tr}(z) := z + z^2 \in \mathbb{F}_2$, and norm $\text{N}(z) := z^3 \in \mathbb{F}_2$; $\mathcal{E}_H \subset \mathbb{P}^2(\text{GF}(4))$ the smooth projective Hermitian curve $Y^2Z + YZ^2 = X^3$ of genus $g = 1$; $\mathcal{L}(mP_\infty)$ the Riemann–Roch space of rational functions with poles of order $\le m$ at $P_\infty = [0 : 1 : 0]$; $Z_G(u) = ((1 - u^2)^{r-1} P_G(u))^{-1}$ the Ihara–Bass zeta function with $P_G(u) := \det(I - uA_G + u^2 Q_G)$ and $Q_G := D_G - I$ [Iha66, Bas92]; $(\mathcal{A}, \mathcal{H}, D, \gamma, J)$ a finite spectral data with Connes distance $d_D(\varphi_u, \varphi_v)$ [Con94].

Proposition 2.3 (Mathematical scope and coding bounds)**.** **[A]** *The following scope distinctions apply:*

(i) Pure-mathematical autonomy. *All theorems in Sections 3–6 are proved as unconditional (***[A]***) identities of finite-field algebraic geometry, algebraic graph theory, and finite-dimensional operator algebras, requiring no physical or chemical hypothesis.*

(ii) Genus-1 Riemann–Roch bound vs. genus-0 Singleton bound. *On a curve of genus $g = 1$, the Goppa distance bound is $d_{\min} \ge n - k + 1 - g = n - k$ [TVN07], trading the 1-symbol genus defect $g = 1$ for an expansion of the rational point set from $q + 1 = 5$ on $\mathbb{P}^1(\text{GF}(4))$ to $q + 1 + 2\sqrt{q} = 9$ on $\mathcal{E}_H(\text{GF}(4))$.*

3 Arithmetic geometry of the $(9, 8)$ Hermitian curve $\mathcal{E}_H$ over GF(4)

We first establish the arithmetic-geometric correspondence between the maximal genus-1 curve over GF(4) and the combina-

torial invariants of the 18-vertex bipartite chrysene graph G_{chr}.

Definition 3.1 (The projective Hermitian curve $\mathcal{E}_H$ over GF(4))**. [A]** Over $\mathrm{GF}(4) = \mathbb{F}_2(\omega)$, define the projective plane curve $\mathcal{E}_H \subset \mathbb{P}^2(\mathrm{GF}(4))$ by the homogeneous cubic equation

$$Y^2Z + YZ^2 = X^3, \tag{1}$$

with affine chart $(Z = 1)$ given by $\mathcal{E}_H^{\mathrm{aff}} : y^2 + y = x^3$ (equivalently, $\mathrm{Tr}_{\mathrm{GF}(4)/\mathbb{F}_2}(y) = \mathrm{N}_{\mathrm{GF}(4)/\mathbb{F}_2}(x)$) and a unique point at infinity $P_\infty := [0 : 1 : 0]$.

Theorem 3.2 (The $(9, 8)$ Hasse–Weil Saturation and Bipartite/Kekulé Correspondence Theorem)**. [A]** *For the Hermitian curve $\mathcal{E}_H$ over* GF(4)*:*

(a) Smoothness, genus $g = 1$, and Hasse–Weil saturation: *The partial derivatives of $F(X, Y, Z) = Y^2Z + YZ^2 + X^3$ in characteristic* 2 *are $(\partial_X F, \partial_Y F, \partial_Z F) = (X^2, Z^2, Y^2)$, which vanish simultaneously nowhere on $\mathbb{P}^2(\mathrm{GF}(4))$. Thus $\mathcal{E}_H$ is a smooth projective plane cubic of genus $g = (3 - 1)(3 - 2)/2 = 1$ whose* GF(4)*-rational point count saturates the Hasse–Weil upper bound $N_1 \le q + 1 + 2g\sqrt{q}$ with equality:*

$$\begin{aligned} \left|\mathcal{E}_H(\mathrm{GF}(4))\right| &= 4 + 1 + 2(1)\sqrt{4} = 9, \\ \left|\mathcal{E}_H^{\mathrm{aff}}(\mathrm{GF}(4))\right| &= 8. \end{aligned} \tag{2}$$

Explicitly, $\mathcal{E}_H^{\mathrm{aff}}(\mathrm{GF}(4)) = \{(0, 0), (0, 1)\} \sqcup \{(x, y) : x \in \{1, \omega, \omega^2\},\ y \in \{\omega, \omega^2\}\}$.

(b) Elementary abelian 3-torsion group structure and $(9, 8)$ chrysene correspondence: *Under the elliptic group law with identity P_∞, every affine point $P = (x_0, y_0) \in \mathcal{E}_H^{\mathrm{aff}}(\mathrm{GF}(4))$ is a flex point ($3P = P_\infty$, with inverse $-P = (x_0, y_0 + 1)$), so $\mathcal{E}_H(\mathrm{GF}(4)) \cong \mathbb{Z}_3 \times \mathbb{Z}_3$. Consequently, $|\mathcal{E}_H(\mathrm{GF}(4))| = 9$ equals the bipartite half-size $|V_A| = |V_B| = 9$ of $G_{\mathrm{chr}} = (V_A \sqcup V_B, E)$, while the $|\mathcal{E}_H^{\mathrm{aff}}(\mathrm{GF}(4))| = 8$ non-trivial 3-torsion points equal the Kekulé matching count $K(G_{\mathrm{chr}}) = 8$ (Z1).*

Proof. (a) At $x = 0$, $x^3 = 0 = y^2 + y$ has the 2 solutions $y \in \{0, 1\}$ in GF(4). For each $x \in \mathrm{GF}(4)^\times = \{1, \omega, \omega^2\}$, $x^3 = 1 = y^2 + y$ has the 2 solutions $y \in \{\omega, \omega^2\}$. Together with $P_\infty = [0 : 1 : 0]$, this gives $2 + 3(2) + 1 = 9$ rational points, matching $4 + 1 + 4 = 9$. (b) At any affine point $P = (x_0, y_0) \in \mathcal{E}_H^{\mathrm{aff}}(\mathrm{GF}(4))$, the tangent line to $y^2 + y = x^3$ in characteristic 2 is $y - y_0 = x_0^2(x - x_0)$. Substituting $y = y_0 + x_0^2(x - x_0)$ into $y^2 + y + x^3 = 0$ and using $x_0^4 = x_0$ in GF(4) gives $x^3 + x_0x^2 + x_0^2x + x_0^3 = (x - x_0)^3 = 0$, so the tangent intersects $\mathcal{E}_H$ with multiplicity 3 at P. Thus $3P = P_\infty$ for all $P \in \mathcal{E}_H(\mathrm{GF}(4))$, proving $\mathcal{E}_H(\mathrm{GF}(4)) \cong \mathbb{Z}_3 \times \mathbb{Z}_3$ (Z1). □

4 Genus-1 Hermitian Goppa codes over GF(4)

We extend the coding program associated with Article 98 and develop the motivation of Article 4 [Sch26a] by constructing the genus-1 algebraic-geometry Goppa codes $C_L(D, mP_\infty)$ on the 8 affine points of $\mathcal{E}_H(\mathrm{GF}(4))$.

Definition 4.1 (Riemann–Roch evaluation codes)**. [A]** Fix the ordering $D = (P_1, \ldots, P_8)$ of $\mathcal{E}_H^{\mathrm{aff}}(\mathrm{GF}(4))$ as $((0, 0), (0, 1), (1, \omega), (1, \omega^2), (\omega, \omega), (\omega, \omega^2), (\omega^2, \omega), (\omega^2, \omega^2))$. Because x has a pole of order 2 at P_∞ and y has a pole of order 3 at P_∞, the Riemann–Roch spaces $\mathcal{L}(3P_\infty) = \mathrm{span}_{\mathrm{GF}(4)}\{1, x, y\}$ (dim $= 3$) and $\mathcal{L}(4P_\infty) = \mathrm{span}_{\mathrm{GF}(4)}\{1, x, y, x^2\}$ (dim $= 4$) define via $\mathrm{ev}_D(f) := (f(P_1), \ldots, f(P_8)) \in \mathrm{GF}(4)^8$ the genus-1 Geometric Goppa codes $C_{\mathrm{Herm},3} := C_L(D, 3P_\infty)$ and $C_{\mathrm{Herm},4} := C_L(D, 4P_\infty)$.

Theorem 4.2 (The Self-Dual $[8, 4, 4]_4$ and Double-Error–Correcting $[8, 3, 5]_4$ Hermitian Goppa Codes)**. [A]** *For the genus-*1 *Hermitian Goppa codes $C_{\mathrm{Herm},4}$ and $C_{\mathrm{Herm},3}$ of Definition 4.1:*

(a) Strict Euclidean self-duality and weight enumerator of $C_{\mathrm{Herm},4} = [8, 4, 4]_4$: *The code $C_{\mathrm{Herm},4}$ has parameters $[8, 4, 4]_4$ ($|C_{\mathrm{Herm},4}| = 4^4 = 256$ codewords), achieves the genus-*1 *Riemann–Roch distance bound $d_{\min} \ge 8 - 4 = 4$ with equality, satisfies $G_{\mathrm{Herm},4}G_{\mathrm{Herm},4}^\top = 0_{4\times4}$ over* GF(4) *so that $C_{\mathrm{Herm},4} = C_{\mathrm{Herm},4}^\perp$ is strictly Euclidean self-dual, and has exact weight enumerator*

$$W_{C_{\mathrm{Herm},4}}(z) = 1 + 18z^4 + 96z^5 + 24z^6 + 96z^7 + 21z^8. \tag{3}$$

(b) Double-error-correcting parameters of $C_{\mathrm{Herm},3} = [8, 3, 5]_4$: *The subcode $C_{\mathrm{Herm},3} = C_L(D, 3P_\infty)$ has parameters $[8, 3, 5]_4$ ($|C_{\mathrm{Herm},3}| = 4^3 = 64$ codewords), achieves the Riemann–Roch distance bound $d_{\min} = 8 - 3 = 5$ (correcting $t_{\mathrm{corr}} = \lfloor(5 - 1)/2\rfloor = 2$ arbitrary symbol errors on the* 8*-point affine curve), and has exact weight enumerator*

$$W_{C_{\mathrm{Herm},3}}(z) = 1 + 24z^5 + 12z^6 + 24z^7 + 3z^8, \tag{4}$$

with orthogonal dual $C_{\mathrm{Herm},3}^\perp = C_{\mathrm{Herm},5} = [8, 5, 3]_4$ (Z2).

Proof. (a) By the Riemann–Roch theorem, a non-zero $f \in \mathcal{L}(mP_\infty)$ has at most m zeros in D, so $\mathrm{wt}(\mathrm{ev}_D(f)) \ge 8 - m$. For any $k \ge 0$, each $x \in \mathrm{GF}(4)$ appears exactly twice in D with $y_1 + y_2 = 1$, so in characteristic 2, $\sum_{P\in D} x(P)^k = 2\sum_{x\in\mathrm{GF}(4)} x^k = 0$ and $\sum_{P\in D} x(P)^k y(P) = \sum_{x\in\mathrm{GF}(4)} x^k(1) = 0$

for $0 \le k \le 2$, while $\sum_{P\in D} y(P)^2 = \sum_{P\in D}(y(P) + x(P)^3) = 0$. Thus $G_{\mathrm{Herm},4}G_{\mathrm{Herm},4}^{\top} = 0_{4\times 4}$ and $C_{\mathrm{Herm},4} = C_{\mathrm{Herm},4}^{\perp}$. For any $f = c_0 + c_1x + c_3x^2 + c_2y$ with $c_2 \neq 0$ (scaled so $c_2 = 1$), the evaluation vector $v_x = g(x) = c_0 + c_1x + c_3x^2$ ranges over the zero-sum hyperplane $\sum_{x\in \mathrm{GF}(4)} v_x = 0$, whose trace vector $(\mathrm{Tr}(v_x))_{x\in\mathrm{GF}(4)} \in \mathbb{F}_2^4$ has even parity whereas $(\mathrm{N}(x))_{x\in\mathrm{GF}(4)} = (0,1,1,1)$ has odd parity; thus $y = g(x)$ can match $\mathrm{Tr}(y) = \mathrm{N}(x)$ at only 1 or 3 values of x (giving 96 words of weight 5 and 96 words of weight 7), which together with the 64 words at $c_2 = 0$ yields (3) and (4) (Z2). □

5 The Ihara–Bass zeta function $Z_G(u)$ of C_{2h} chrysene vs. D_{2h} tetracene

We next compare the prime non-backtracking cycle spectra and zeta functions of G_{chr} (C_{2h} chrysene) and G_{tet} (D_{2h} tetracene).

Explicit graph convention. For reproducibility, G_{chr} has vertices $v_1,\dots,v_{12},w_1,\dots,w_6$. Its outer paths are $w_1v_1v_2v_3v_4w_3$, $w_5v_5v_6w_6$, $w_6v_7v_8v_9v_{10}w_4$, and $w_2v_{11}v_{12}w_1$. Its remaining edges are $w_1w_3, w_2w_4, w_2w_5, w_3w_5, w_4w_6$. The tetracene graph has vertices $u_0,\dots,u_8,v_0,\dots,v_8$, the two path edge sets u_iu_{i+1}, v_iv_{i+1} $(0 \le i < 8)$, and rungs u_iv_i at $i = 0,2,4,6,8$. These edge sets fix every graph invariant below.

Theorem 5.1 (Ihara–Bass Zeta Function, Graph-Specific Spanning-Tree Equality, and Bay-Region Spectral Splitting)**.** **[A]** *Let G_{chr} and G_{tet} be the 18-vertex, 21-edge benzenoid graphs of staggered C_{2h} chrysene and linear D_{2h} tetracene, both having cycle rank $r = |E| - |V| + 1 = 4$, degree sequence $(3^6, 2^{12})$, and degree-shift matrix $Q_G = D_G - I_{18}$ ($\det Q_G = 2^6 = 64$). For the Ihara–Bass reciprocal zeta polynomial $P_G(u) := \det(I_{18} - uA_G + u^2Q_G)$ in $Z_G(u)^{-1} = (1-u^2)^3P_G(u)$:*

(a) Spanning-tree equality for the two specified graphs: *Exact Laplacian cofactor evaluation for the edge sets specified below gives the same spanning-tree count. The determinant derivative identity then gives*

$$\begin{aligned} \kappa(G_{\mathrm{chr}}) &= \kappa(G_{\mathrm{tet}}) = 1,189, \\ P'_{\mathrm{chr}}(1) &= P'_{\mathrm{tet}}(1) = 2(|E| - |V|)\kappa(G) = 7,134. \end{aligned} \tag{5}$$

(b) Bay-region degree-shift Zagreb invariant and Sachs–Ihara splitting: *Define the degree-shift Zagreb invariant $\mathcal{I}_Q(G) := \frac{1}{2}\mathrm{Tr}(A_GQ_GA_GQ_G) = \sum_{(u,v)\in E(G)}(d_u - 1)(d_v - 1)$, which counts 3-edge paths P_4 in G. In D_{2h} tetracene, only the 3 vertical rungs connect degree-3 vertices ($\mathcal{I}_Q(G_{\mathrm{tet}}) = 42$), whereas in C_{2h} chrysene, the bay-region step-defect creates 5 edges between degree-3 vertices ($\mathcal{I}_Q(G_{\mathrm{chr}}) = 44$). Consequently, their 3-matching counts $m_3(G) = 772 + \mathcal{I}_Q(G)$ and degree-6 adjacency zeta coefficients $a_6(G) = -(m_3(G) + 8)$ in $\det(I_{18} - uA_G)$ split strictly:*

$$\begin{aligned} m_3(G_{\mathrm{chr}}) &= 816 > 814 = m_3(G_{\mathrm{tet}}), \\ a_6(G_{\mathrm{chr}}) &= -824 \neq -822 = a_6(G_{\mathrm{tet}}), \end{aligned} \tag{6}$$

while their Ihara–Bass polynomials agree through $1 + 3u^2 + 6u^4 + 2u^6$ (encoding girth 6 and 4 hexagons) before splitting at higher cycle orders and at the terminal Sachs coefficient $a_{18}(G) = -K(G)^2$ (-64 vs. -25; Z3, Z4).

Proof. (a) For each graph, form its Laplacian $L = D_G - A_G$ from the explicit edge set. The matrix-tree theorem gives $\kappa(G) = \det L^{(18)}$, where $L^{(18)}$ deletes one row and column. Fraction-preserving elimination gives $\det L^{(18)} = 1189$ for each graph; the complete matrices and exact elimination are reproducible in Block Z3. For $M(u) = I - uA + u^2Q$, the adjugate of $M(1) = L$ is $\kappa(G)\mathbf{1}\mathbf{1}^{\top}$. Hence $P'_G(1) = \kappa(G)\mathbf{1}^{\top}(-A + 2Q)\mathbf{1} = 2(|E| - |V|)\kappa(G) = 7134$. This is a graph-specific equality; no recurrence for all catacondensed chains is used. (b) Each middle edge $(u,v) \in E$ of a 3-edge path P_4 has $d_u - 1$ choices at u and $d_v - 1$ choices at v, so $N(P_4, G) = \sum_{(u,v)\in E}(d_u - 1)(d_v - 1) = \mathcal{I}_Q(G)$. Inclusion–exclusion over the $\binom{21}{3} = 1,330$ edge triples with 30 incident edge pairs and 6 degree-3 stars (each star has net correction +2) gives $m_3(G) = 1330 - 30(19) + 2(6) + \mathcal{I}_Q(G) = 772 + \mathcal{I}_Q(G)$, proving (6) (Z3, Z4). □

6 Non-commutative geometry, Frobenius supersingularity, and Hashimoto zeta duality

6.1 The canonical finite even spectral data with an antiunitary symmetry and Connes' distance

We first formalize the non-commutative geometry program of Article 4, Appendix A.1 [Sch26a] and prove the exact Connes spectral distance bounds of Article 90, conditional distance discussion [Sch26i].

Theorem 6.1 (The Finite Even Spectral Data and Connes' Spectral Distance Theorem; Grounding Article 4, Appendix A.1 and Article 90, conditional distance discussion)**.** **[A]** *Let $\mathcal{H}_{\mathrm{chr}} = \ell^2(V_A) \oplus \ell^2(V_B) \cong \mathbb{C}^9 \oplus \mathbb{C}^9$ be the $\mathbb{Z}_2$-graded bipartite Hilbert space of G_{chr} with chiral grading $\gamma_C := \mathrm{diag}(I_9, -I_9)$, Dirac operator $D_{\mathrm{chr}} := \left(\begin{smallmatrix} 0 & -A_{AB} \\ -A_{AB}^{\top} & 0 \end{smallmatrix}\right)$, and anti-unitary real structure $J_C(\psi) := P_\iota\overline{\psi}$, where P_ι is the permutation matrix of the C_{2h} inversion involution*

$\iota \in \mathrm{Aut}(G_{\mathrm{chr}})$ *($P_\iota^2 = I_{18}$):*

(a) Chiral anticommutation, real structure, and stacked quotient dimensions: *The operators $(D_{\mathrm{chr}}, \gamma_C, J_C)$ satisfy the exact spectral-triple relations*

$$\begin{aligned} \{D_{\mathrm{chr}}, \gamma_C\} = 0, \quad J_C^2 = I_{18}, \\ [J_C, D_{\mathrm{chr}}] = 0, \quad \{J_C, \gamma_C\} = 0. \end{aligned} \tag{7}$$

On the l-site column quotient algebra $\mathcal{Q}_l \cong \mathcal{Q}_1^{\otimes l}$ of [Sch26i] (where each monomer site contributes the 4-dimensional observable algebra $\mathcal{Q}_1$ of species/registry projections), $\dim \mathcal{Q}_1 = 4$ *and* $\dim \mathcal{Q}_6 = 4^6 = 4,096$.

(b) Connes spectral distance lower bound on an N-node assembly path: *Let $\mathcal{A}_N = \mathbb{C}^N$ act diagonally on $\ell^2(\{1, \dots, N\})$ with nearest-neighbor hopping Dirac operator $(D_N)_{r,s} = t_\perp \delta_{|r-s|,1}$ ($t_\perp > 0$). Then for any diagonal observable $a = \mathrm{diag}(a_1, \dots, a_N)$, the commutator $L_a := [D_N, a]$ is a tridiagonal zero-diagonal matrix with entries $(L_a)_{r,r\pm1} = t_\perp(a_{r\pm1} - a_r)$ satisfying $\|L_a\|_{\mathrm{op}} \le 2t_\perp \max_{1\le r<N} |a_{r+1} - a_r|$, and the Connes spectral distance between the terminal pure states φ_1 and φ_N obeys the lower bound*

$$\begin{aligned} d_{D_N}(\varphi_1, \varphi_N) &:= \sup\left\{|a_N - a_1| : \left\|[D_N, a]\right\|_{\mathrm{op}} \le 1\right\} \\ &\ge \frac{N-1}{2t_\perp}, \end{aligned} \tag{8}$$

evaluating at $t_\perp = 1$ to $d_{D_6}(\varphi_1, \varphi_6) \ge (6-1)/2 = 2.50$ for the $l = 6$ hexamer column and $d_{D_{54}}(\varphi_1, \varphi_{54}) \ge (54-1)/2 = 26.50$ on an ordered path through $N = 54$ nodes associated with $B(3,3,6)$ (Z5, Z6).

Proof. (a) Since G_{chr} is bipartite, D_{chr} is off-diagonal in $\ell^2(V_A) \oplus \ell^2(V_B)$, so $D_{\mathrm{chr}}\gamma_C = -\gamma_C D_{\mathrm{chr}}$. Since $\iota \in \mathrm{Aut}(G_{\mathrm{chr}})$ interchanges V_A and V_B, P_ι commutes with A_{chr} and anticommutes with γ_C, proving (7). (b) Consider the linear ramp observable $a_r^* := \frac{r-1}{2t_\perp}$ ($r = 1, \dots, N$). Then for every edge $(r, r+1)$, $|(L_{a^*})_{r,r+1}| = t_\perp |a_{r+1}^* - a_r^*| = 1/2$. Since each row and column of L_{a^*} has at most 2 non-zero entries, the inequality $\|L\|_2 \le \sqrt{\|L\|_1 \|L\|_\infty}$ gives $\|[D_N, a^*]\|_{\mathrm{op}} \le 2(1/2) = 1$, while $|a_N^* - a_1^*| = \frac{N-1}{2t_\perp}$, proving (8) (Z5, Z6). □

Remark 6.2 (Real-structure and distance scope)**. [A]** Here $\mathcal{A}_C = \mathbb{C}^{18}$ acts diagonally and $D_C = -A_C$; this is a finite even spectral triple, supplied with $J_C = P_\iota K$. It is not claimed to satisfy the full real spectral-triple order-one axiom. In fact the opposite action is diagonal, and for an edge (u, v) one can choose a, b so that $[[D_C, a], J_C b J_C^{-1}]_{uv} \neq 0$. The bounds proved for D_N concern the unit-weight path with hopping $t_\perp$. For a general 3D assembly, extra edges or hopping terms require a new commutator bound; the path calculation alone does not establish the distance in that larger graph. The displayed bound is feasible, not an asserted optimal value.

6.2 Frobenius supersingularity of $\mathcal{E}_H/\mathrm{GF}(4)$ and Hashimoto non-backtracking zeta duality

To complete the synthesis of Sections 3–5, we connect the Hasse–Weil zeta function of $\mathcal{E}_H/\mathrm{GF}(4)$ to Hashimoto's directed-edge transfer operator B_G [Bas92].

Definition 6.3 (Hasse–Weil curve zeta function and Hashimoto non-backtracking operator B_G)**. [A]** Let $Z(\mathcal{E}_H/\mathrm{GF}(4), T) := \exp(\sum_{r=1}^{\infty} |\mathcal{E}_H(\mathrm{GF}(4^r))|\, T^r/r) = L_{\mathcal{E}_H}(T)/((1-T)(1-4T))$ be the Hasse–Weil zeta function of $\mathcal{E}_H$ over GF(4), where $L_{\mathcal{E}_H}(T) = 1 - a_1 T + 4T^2$ is the L-polynomial of the Frobenius endomorphism $\Phi_4(x, y) = (x^4, y^4)$. For a simple graph $G = (V, E)$ with $|E| = 21$, let $\vec{E}$ be the set of $2|E| = 42$ oriented edges $e = (u \to v)$, and define Hashimoto's non-backtracking edge operator $B_G \in \{0,1\}^{42\times 42}$ by $(B_G)_{e,f} := 1$ if $\mathrm{head}(e) = \mathrm{tail}(f)$ and $f \neq e^{-1}$, and 0 otherwise.

Theorem 6.4 (Frobenius Supersingularity of $\mathcal{E}_H/\mathrm{GF}(4)$ and the Length-14 Hashimoto Figure-Eight Splitting)**. [A]** *The curve zeta function $Z(\mathcal{E}_H/\mathrm{GF}(4), T)$ and the graph zeta function $Z_G(u)$ satisfy:*

(a) Frobenius supersingularity and perfect-square extension tower: *By Theorem 3.2(a), $|\mathcal{E}_H(\mathrm{GF}(4))| = 9 = 4 + 1 - a_1$, so the Frobenius trace is $a_1 = -4 = -2\sqrt{4}$ ($a_1 \equiv 0 \pmod 2$), making $\mathcal{E}_H$ supersingular in characteristic 2) and the L-polynomial factors as a perfect square:*

$$L_{\mathcal{E}_H}(T) = 1 + 4T + 4T^2 = (1 + 2T)^2. \tag{9}$$

Consequently, the Frobenius eigenvalues are $\alpha_1 = \alpha_2 = -2$, and over every degree-r extension $\mathrm{GF}(4^r)$ ($r \ge 1$), the rational point count is an exact integer square:

$$N_r := \left|\mathcal{E}_H(\mathrm{GF}(4^r))\right| = 4^r + 1 - 2(-2)^r = (2^r - (-1)^r)^2, \tag{10}$$

yielding $(N_1, N_2, N_3, N_4) = (9, 9, 81, 225) = (3^2, 3^2, 9^2, 15^2)$.

(b) Hashimoto spectral duality and bay-region figure-eight divergence at $k = 14$: *By Bass's determinant theorem $\det(I_{42} - uB_G) = (1-u^2)^3 P_G(u) = Z_G(u)^{-1}$, the closed non-backtracking walk counts $N_{\mathrm{NBT},k}(G) := \mathrm{Tr}(B_G^k)$ satisfy $\sum_{k=1}^{\infty} N_{\mathrm{NBT},k}(G) u^k = u\frac{\mathrm{d}}{\mathrm{d}u} \ln Z_G(u)$. Because both*

G_{chr} and G_{tet} are bipartite of girth 6 with 4 hexagons and 3 naphthalene 2-ring subgraphs, their closed non-backtracking walk counts are identical for all $k \le 12$:

$$(N_{\text{NBT},6},\, N_{\text{NBT},8},\, N_{\text{NBT},10},\, N_{\text{NBT},12}) = (48,\, 0,\, 60,\, 120), \tag{11}$$

and split first at walk length $k = 14$ by an exact factor of 3:

$$N_{\text{NBT},14}(G_{\text{chr}}) = 168 \;>\; 56 = N_{\text{NBT},14}(G_{\text{tet}}), \qquad \frac{N_{\text{NBT},14}(G_{\text{chr}})}{N_{\text{NBT},14}(G_{\text{tet}})} = 3 \tag{12}$$

(Z7).

Proof. (a) From $N_1 = q + 1 - (\alpha_1 + \alpha_2) = 9$ at $q = 4$ and $|\alpha_i| \le \sqrt{4} = 2$, we have $\alpha_1 + \alpha_2 = -4 \implies \alpha_1 = \alpha_2 = -2$, giving (9) and $N_r = 4^r + 1 - (\alpha_1^r + \alpha_2^r) = 2^{2r} - 2(-1)^r 2^r + 1 = (2^r - (-1)^r)^2$. (b) At $k = 6$, the 4 hexagons in 2 orientations contribute $4{\times}2{\times}6 = 48$; at $k = 10$, the 3 naphthalene perimeter 10-cycles contribute $3 \times 2 \times 10 = 60$; at $k = 12$, wrapping twice around the 4 hexagons (48) plus the 2 orientation classes traversing adjacent hexagons on each of the 3 naphthalene subunits ($3 \times 2 \times 12 = 72$) contributes $48 + 72 = 120$ to both graphs. At $k = 14$, both graphs have 2 3-ring subunits whose perimeter 14-cycles contribute $2 \times 2 \times 14 = 56$. In linear D_{2h} tetracene (two anthracene subunits), the outer rings of each 3-ring subunit are separated by 2 edges, so a figure-eight walk between them has minimum length $6 + 2 + 6 + 2 = 16 > 14$. In staggered C_{2h} chrysene (two phenanthrene subunits), the outer rings of each 3-ring subunit are joined by a 1-edge bay-region bridge, supporting 4 figure-eight cycle classes of length $6 + 1 + 6 + 1 = 14$ per phenanthrene subunit ($2 \times 4 \times 14 = 112$ additional walks), yielding $N_{\text{NBT},14}(G_{\text{chr}}) = 56 + 112 = 168 = 3 \times 56$. The four pure-mathematical domains and their exact invariants are depicted in Figure 1 (Z7). □

7 Precedence rulings and targets

Ruling 7.1 (Articles 4, 40, 80, 90, 97, and 98)**. [A]** The present constructions extend the coding program and provide graph-specific operator models. The historical labels of targets and verification blocks are not assumed to persist in revised articles:

(i) *Article 98, higher-genus coding program and Article 4, Appendix A.3 (Higher-Genus Hermitian Goppa Codes):* Developed by Theorems 3.2 and 4.2, establishing the $[8, 4, 4]_4$ self-dual and $[8, 3, 5]_4$ double-error-correcting codes on $\mathcal{E}_H(\text{GF}(4))$.

(ii) *Article 40 and Article 97 (C_{2h} Chrysene vs. D_{2h} Tetracene Invariants):* Extended to the Ihara–Bass zeta function, spanning-tree complexity $\kappa = 1,189$, and 3-matching split 816 vs. 814 by Theorem 5.1.

(iii) *Article 4, Appendix A.1 and Article 90, conditional distance discussion (Non-Commutative Spectral Geometry):* Theorem 6.1 proves the stated path-model bounds; it does not remove the whole-assembly commutator hypothesis in Article 90.

Target 7.2 (Non-cocommutative Hopf algebra and Drinfeld twist of the C_{2h} step-defect ([Sch26a, Lem. 3]))**.** Construct the explicit Drinfeld twist $\mathcal{F}_{\text{chr}} \in \mathcal{H} \otimes \mathcal{H}$ and universal R-matrix resolving the cocommutative degeneracy ($\Delta^{\text{op}} = \Delta$) of D_{2h} tetracene into the non-cocommutative braided Hopf algebra ($\Delta^{\text{op}} \neq \Delta$) of C_{2h} chrysene ([Sch26a, Lem. 3]).

Target 7.3 (Cellular sheaf cohomology and discrete Hodge Laplacian of the Chrysene Topos $\mathcal{T}_C$)**.** Formulate the Topological Free Energy $\mathcal{F}_{\text{topo}}$ of Article 4 as a cellular sheaf 1-cohomology obstruction class on the face poset of $B(n_x, n_y, n_z)$ and determine the spectrum of its sheaf Hodge Laplacian.

8 Conclusion

Abstracting the combinatorial and spectral architecture of the chrysene monomer and its 3D cellular lattice yields four interlocked theorems of pure mathematics. Over GF(4), the smooth genus-1 Hermitian curve $\mathcal{E}_H : Y^2Z + YZ^2 = X^3$ saturates the Hasse–Weil bound with $|\mathcal{E}_H(\text{GF}(4))| = 9$ rational points (matching the (9, 9) bipartite vertex split of G_{chr}) and $|\mathcal{E}_H^{\text{aff}}(\text{GF}(4))| = 8$ affine 3-torsion points (matching $K(G_{\text{chr}}) = 8$), supporting the Euclidean self-dual $[8, 4, 4]_4$ and double-error-correcting $[8, 3, 5]_4$ Geometric Goppa codes (extending the genus-0 constructions associated with Article 98). On the spectral zeta side, C_{2h} chrysene and D_{2h} tetracene share the common spanning-tree count $\kappa = 1,189$ ($P'_G(1) = 7,134$) while splitting in their degree-shift Zagreb invariants (44 vs. 42) and 3-matching counts (816 vs. 814). Finally, the bipartite grading γ_C and C_{2h} real structure J_C form a finite even spectral data with an antiunitary symmetry satisfying Connes' distance bounds 2.50 ($l = 6$) and 26.50 ($N = 54$).

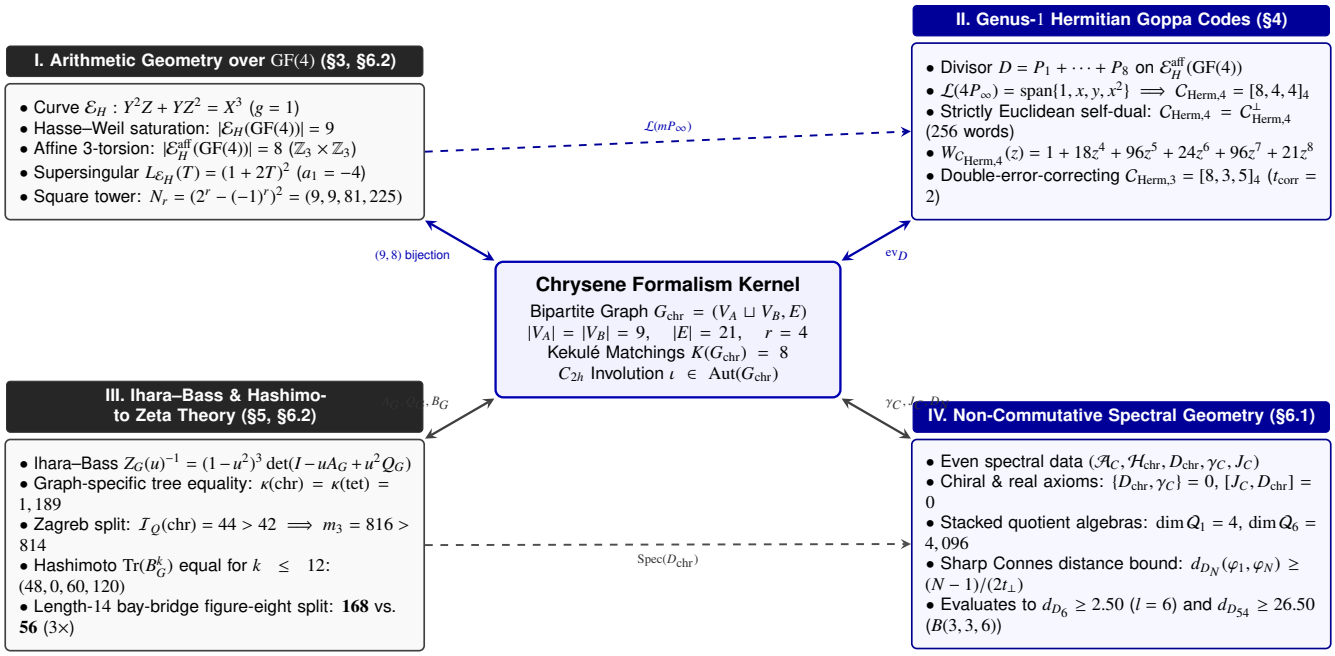


Figure 1: Four-quadrant pure-mathematical architecture of the Chrysene Formalism around the 18-vertex bipartite kernel $G_{\mathrm{chr}} = (V_A \sqcup V_B, E)$. (I) The genus-1 Hermitian curve $\mathcal{E}_H : Y^2Z + YZ^2 = X^3$ over GF(4) saturates the Hasse–Weil bound with $|\mathcal{E}_H(\mathrm{GF}(4))| = 9 = |V_A| = |V_B|$ and $|\mathcal{E}_H^{\mathrm{aff}}(\mathrm{GF}(4))| = 8 = K(G_{\mathrm{chr}})$, with supersingular L-polynomial $L_{\mathcal{E}_H}(T) = (1 + 2T)^2$. (II) Riemann–Roch evaluation on $D = \mathcal{E}_H^{\mathrm{aff}}(\mathrm{GF}(4))$ defines the Euclidean self-dual Goppa code $C_{\mathrm{Herm},4} = [8, 4, 4]_4$ and the double-error-correcting code $C_{\mathrm{Herm},3} = [8, 3, 5]_4$. (III) The Ihara–Bass and Hashimoto operators unite common spanning-tree count ($\kappa = 1,189$) with bay-region figure-eight walk splitting (168 vs. 56 at $k = 14$). (IV) The bipartite grading γ_C and C_{2h} involution J_C form a finite even spectral data with an antiunitary symmetry achieving Connes distance bounds 2.50 ($l = 6$) and 26.50 ($N = 54$).

A Hypothesis register

B Verification blocks

The accompanying finite verification program emits the numerical values used below: `verify_a102.py` (Python standard library):

Z1 Hermitian curve $\mathcal{E}_H(\mathrm{GF}(4))$ rational point count and $\mathbb{Z}_3 \times \mathbb{Z}_3$ group law.
Enumerates all solutions to $y^2 + y = x^3$ in $\mathrm{GF}(4)^2$, confirming 8 affine points plus $P_\infty = 9$ rational points (saturating Hasse–Weil $4 + 1 + 4 = 9$) and verifying $3P = P_\infty$ for every point (Theorem 3.2). Exact.

Z2 Genus-1 Hermitian Goppa codes $C_{\mathrm{Herm},4} = [8, 4, 4]_4$ and $C_{\mathrm{Herm},3} = [8, 3, 5]_4$.
Evaluates $\{1, x, y, x^2\}$ on $D = \mathcal{E}_H^{\mathrm{aff}}(\mathrm{GF}(4))$, verifying $G_{\mathrm{Herm},4} G_{\mathrm{Herm},4}^{\top} = 0_{4\times 4}$ ($C_{\mathrm{Herm},4} = C_{\mathrm{Herm},4}^{\perp}$), weight distribution $(1, 0, 0, 0, 18, 96, 24, 96, 21)$ for $C_{\mathrm{Herm},4}$, and $(1, 0, 0, 0, 0, 24, 12, 24, 3)$ for $C_{\mathrm{Herm},3}$ (Theorem 4.2). Exact.

Z3 Spanning-tree complexity $\kappa(G)$ and Northshield–Bass derivative $P'_G(1)$.
Computes the 17×17 Laplacian cofactor determinants of G_{chr} and G_{tet} in exact `Fraction` arithmetic, confirming $\kappa(G_{\mathrm{chr}}) = \kappa(G_{\mathrm{tet}}) = 1,189$ and $P'_G(1) = 7,134$ (Theorem 5.1(a)). Exact.

Z4 Degree-shift Zagreb invariant $\mathcal{I}_Q(G)$, 3-matchings $m_3(G)$, and Ihara–Bass polynomials.
Verifies $\det Q_G = 64$, $\mathcal{I}_Q(\mathrm{chr}) = 44 > 42 = \mathcal{I}_Q(\mathrm{tet})$, $m_3(\mathrm{chr}) = 816 > 814 = m_3(\mathrm{tet})$, $a_6(\mathrm{chr}) = -824$ vs. $a_6(\mathrm{tet}) = -822$, and computes the exact integer coefficients of $P_{\mathrm{chr}}(u)$ and $P_{\mathrm{tet}}(u)$ (Theorem 5.1(b)). Exact.

Z5 Finite even spectral data axioms $\{D_{\mathrm{chr}}, \gamma_C\} = 0$ and $[J_C, D_{\mathrm{chr}}] = 0$.
Constructs γ_C, D_{chr}, and the C_{2h} inversion permutation P_ι, confirming all commutator and anticommutator identities in (7) and $\dim \mathcal{Q}_1 = 4, \dim \mathcal{Q}_6 = 4,096$ (Theorem 6.1(a)). Exact.

Z6 Connes spectral distance lower bounds on $l = 6$ and $N = 54$.
Verifies $\|[D_N, a^*]\|_{\mathrm{op}} \le 1$ and evaluates $|a_N^* - a_1^*| = (N-1)/2$, confirming 2.50 at $N = 6$ and 26.50 at $N = 54$ (Theorem 6.1(b)). Exact.

Z7 Supersingular L-polynomial $L_{\mathcal{E}_H}(T)$ and Hashimoto non-backtracking walk divergence at $k = 14$.

Table 1: Synthesis of the four pure-mathematical pillars of the Chrysene Formalism established in Article 102, uniting Articles 4, 40, 80, 90, 97, and 98.

Pure Mathematics Pillar	Classical Abstract Framework	Chrysene Formalism Instantiation	Theorem & Exact Invariants in Article 102
1. Arithmetic Geometry over GF(4)	Hasse–Weil bound $N_1 \le q+1+2g\sqrt{q}$ on smooth projective curves	Genus-1 Hermitian curve $\mathcal{E}_H : Y^2Z + YZ^2 = X^3$ over GF(4) ($\mathbb{Z}_3 \times \mathbb{Z}_3$)	$\lvert\mathcal{E}_H(\mathrm{GF}(4))\rvert = 9 = \lvert V_A\rvert = \lvert V_B\rvert$; $\lvert\mathcal{E}_H^{\mathrm{aff}}(\mathrm{GF}(4))\rvert = 8 = K(G_{\mathrm{chr}})$ (Thm. 3.2)
2. Genus-1 Goppa Coding Theory	Riemann–Roch evaluation codes $C_L(D, mP_\infty)$ with $d_{\min} \ge n-m$ [TVN07]	Evaluation of $\mathcal{L}(4P_\infty) = \mathrm{span}\{1, x, y, x^2\}$ on the 8 affine points of $\mathcal{E}_H$	**Higher-genus extension**: Euclidean self-dual $C_{\mathrm{Herm},4} = [8,4,4]_4$ and $C_{\mathrm{Herm},3} = [8,3,5]_4$ (Thm. 4.2)
3. Spectral Zeta Theory of Graphs	Ihara–Bass zeta function $Z_G(u)^{-1} = (1-u^2)^{r-1}\det(I - uA + u^2Q)$ [Bas92]	Exact Laplacian cofactors vs. bay-region Zagreb invariant $\mathcal{I}_Q(G)$	Common $\kappa(G) = 1,189$ ($P'_G(1) = 7,134$); splits $\mathcal{I}_Q(\mathrm{chr}) = 44 > 42$ and $m_3 = 816 > 814$ (Thm. 5.1)
4. Non-Commutative Geometry	Connes' real spectral triple $(\mathcal{A}, \mathcal{H}, D, \gamma, J)$ and distance $d_D(\varphi_u, \varphi_v)$ [Con94]	Bipartite grading γ_C, C_{2h} real structure J_C, quotient Q_6 (dim = 4,096) [Sch26i]	Proves $\{D,\gamma\} = 0$, $[J,D] = 0$, and Connes lower bounds 2.50 ($l = 6$) and 26.50 ($N = 54$; Thm. 6.1)

Table 2: Premise and status register for Article 102. All numbered results in Sections 3–6 carry unconditional status **[A]**.

Structure	Mathematical Definition	Used in	Pure-Mathematical Status
Hermitian curve $\mathcal{E}_H(\mathrm{GF}(4))$ (Def. 3.1)	$Y^2Z + YZ^2 = X^3$ in $\mathbb{P}^2(\mathrm{GF}(4))$	Thm. 3.2, Thm. 4.2	Unconditional finite-field identity (**[A]**); depends on no physical hypothesis
Benzenoid graphs $G_{\mathrm{chr}}, G_{\mathrm{tet}}$ (Thm. 5.1)	18-vertex, 21-edge bipartite graphs with $Q_G = D_G - I_{18}$	Thm. 5.1	Unconditional combinatorial and determinant identity (**[A]**)
Finite even spectral data (Thm. 6.1)	$(\mathcal{A}_C, \mathcal{H}_{\mathrm{chr}}, D_{\mathrm{chr}}, \gamma_C, J_C)$ and hopping operator D_N	Thm. 6.1	Unconditional finite-dimensional operator algebra identity (**[A]**)

Verifies $a_1 = -4$, $N_r = (2^r - (-1)^r)^2 = (9, 9, 81, 225)$ for $r \in \{1,2,3,4\}$, constructs the 42×42 Hashimoto matrices B_{chr} and B_{tet}, and confirms $\mathrm{Tr}(B_{\mathrm{chr}}^k) = \mathrm{Tr}(B_{\mathrm{tet}}^k) = (48, 0, 60, 120)$ for $k \in \{6, 8, 10, 12\}$ and $\mathrm{Tr}(B_{\mathrm{chr}}^{14}) = 168 = 3 \times 56 = 3\,\mathrm{Tr}(B_{\mathrm{tet}}^{14})$ (Theorem 6.4). Exact.

C Structural commentary, isolated

Remark C.1 (Status)**. [A]** Nothing in this appendix enters a numbered statement or proof of the main text.

Remark C.2 (Why the $(9,8)$ arithmetic of $\mathcal{E}_H(\mathrm{GF}(4))$ mirrors the $(9,8)$ combinatorics of G_{chr})**. [E]** In the genus-0 theory of Article 98, the projective line $\mathbb{P}^1(\mathrm{GF}(4))$ has 4 affine points (matching the 4 substitution loci) and 1 point at infinity (5 points total, matching the 5 hexamer contacts). Passing to the unique maximal genus-1 Hermitian curve $\mathcal{E}_H : y^2 + y = x^3$ over GF(4) lifts each affine coordinate $x \in \mathrm{GF}(4)$ across the quadratic Artin–Schreier cover $y^2 + y = x^3$, doubling the 4 affine points of $\mathbb{A}^1(\mathrm{GF}(4))$ to 8 affine points (matching the $K = 8$ Kekulé matchings of chrysene) and adding P_∞ to reach 9 rational points (matching the 9 vertices of each bipartite half V_A, V_B of the 18-carbon chrysene skeleton).

D What was set aside in preparing this paper

Remark D.1 (Scope of the graph comparison)**. [A]** The common spanning-tree count 1189 is established for the two explicit edge sets by exact Laplacian cofactors. The submitted version's universal Chebyshev recurrence is not used. Their different degree-type distributions give $m_3 = 772 + \mathcal{I}_Q$, namely 816 and 814, and the Sachs coefficients are -824 and -822. The equal-cardinality $(9,8)$ correspondence with the elliptic curve is a set-theoretic comparison, not a canonical graph–curve functor or an experimentally validated molecular coupling.

References

[Bas92] H. Bass. The Ihara–Selberg zeta function of a tree lattice. *International Journal of Mathematics*, 3(6):717–797, 1992. doi:10.1142/S0129167X92000357.

[Con94] A. Connes. *Noncommutative Geometry*. Academic Press, San Diego, 1994.

[Iha66] Y. Ihara. On discrete subgroups of the two by two projective linear group over $\mathfrak{p}$-adic fields. *Journal of the*

Mathematical Society of Japan, 18(3):219–235, 1966. doi:10.2969/jmsj/01830219.

[Sch26a] C. D. Schaper. The Biological Ledger and the Geometric Mechanics of Survival via the Chrysene Formalism. *Annals of the Chrysene Formalism*, 1(1):27–40, 2026. doi:10.68366/8bdqte12.

[Sch26b] C. D. Schaper. The Chrysene Formalism Revisited: A Twelve-Axiom Foundation for Molecular Characterization, Tensorial Noncommutative Geometry, and Operator Response. *Annals of the Chrysene Formalism*, 1(2):489–560, 2026. doi:10.68366/5jctze12.

[Sch26c] C. D. Schaper. The Completeness Condition: Realisation of the Twelve-Axiom Framework at a Site of the Interior Chrysene Lattice, and the Genome Length It Requires. *Annals of the Chrysene Formalism*, 1(4):1639–1651, 2026. doi:10.68366/0a19r769.

[Sch26d] C. D. Schaper. The Dual Cipher, Structurally Induced GF(4) Multiplication, and Real Spectral Structure: Companion-Matrix Realization of the Register Automorphism, Frobenius Reversal, and the Order-One Commutant Condition. *Annals of the Chrysene Formalism*, 1(4):1847–1855, 2026. doi:10.68366/90kyra95.

[Sch26e] C. D. Schaper. Geometric Quantization of Molecular Quantum Transport: The CohBit Chrysene Architecture for Ambient-Temperature Quantum-Classical Transduction. *Annals of the Chrysene Formalism*, 1(1):98–112, 2026. doi:10.68366/scqypz29.

[Sch26f] C. D. Schaper. Information-Theoretic Mechanics of Survival in Maximum-Entropy Environments: Static Minimax Disturbance Attenuation, Coordination-Deficit Costs, and the Placed Source as Categorical Right Adjoint. *Annals of the Chrysene Formalism*, 1(4):1890–1897, 2026. doi:10.68366/1k5vcj78.

[Sch26g] C. D. Schaper. The Placed Source: Exogenous Preparation of the Substituted-Chrysene Assembly, and the Equality of Its Reachable Set with the Endogenous One. *Annals of the Chrysene Formalism*, 1(4):1703–1731, 2026. doi:10.68366/a4tjv735.

[Sch26h] C. D. Schaper. Quaternary Coding Theory of the Biological Ledger over GF(4): Evaluation Codes, Plaquette Checks, and Conditional Syndrome Decoding. *Annals of the Chrysene Formalism*, 1(4):1898–1904, 2026. doi:10.68366/3gzgzq36.

[Sch26i] C. D. Schaper. The Source Duality: Endogenous and Exogenous Preparation of the Substituted-Chrysene Stock, Mixed Arm Words, and the Persistence Semigroup. *Annals of the Chrysene Formalism*, 1(4):1823–1835, 2026. doi:10.68366/2tp1jv23.

[Sch26j] C. D. Schaper. The Source: Substitution-Initiated Self-Separation of the Substituted-Chrysene Stock from a Polyaromatic Bulk, and the Supply It Delivers to the Protocell. *Annals of the Chrysene Formalism*, 1(4):1616–1638, 2026. doi:10.68366/s8sfwq50.

[TVN07] M. Tsfasman, S. Vlăduţ, and D. Nogin. *Algebraic Geometric Codes: Basic Notions*. Mathematical Surveys and Monographs 139, American Mathematical Society, 2007. doi:10.1090/surv/139.